Edaravone Protects HT22 Neurons from H_2O_2-Induced Apoptosis by Inhibiting the MAPK Signaling Pathway

Zhong-Yan Zhao,[1,2] Ping Luan,[3] Shi-Xiong Huang,[2] Song-Hua Xiao,[1] Jia Zhao,[1] Bei Zhang,[1] Bei-Bei Gu,[1] Rong-Biao Pi[4] & Jun Liu[1]

1 Department of Neurology, Sun Yat-sen Memorial Hospital, Sun Yat-sen University, Guangzhou, Guangdong, China
2 Department of Neurology, Hainan Provincial People's Hospital, Haikou, Hainan, China
3 School of Medicine, Shenzhen University, Shenzhen, Guangdong, China
4 Department of Pharmacology & Toxicology, School of Pharmaceutical Sciences, Sun Yat-Sen University, Guangzhou, China

The first two authors contributed equally to this work.

SUMMARY

Aims: Oxidative stress is frequently implicated in the pathology of neurodegenerative diseases. This study aimed to investigate the effects and their underlying mechanism(s) of edaravone upon hydrogen peroxide (H_2O_2)–induced oxidative stress and apoptosis in HT22 cells, a murine hippocampal neuronal model. **Methods:** HT22 cells were treated with H_2O_2 in the presence of various concentrations of edaravone or in its absence. A CCK-8 assay, Hoechst 33342 staining, and flow cytometry were used to detect cytotoxicity and apoptosis. In addition, the levels of reactive oxygen species (ROS) and the expression of Bcl-2, Bax, p-ERK 1/2, p-JNK, and p-P38 proteins in HT22 cells were examined. **Results:** Exogenous H_2O_2 decreased cell viability in a concentration-dependent manner and was associated with increased apoptosis and ROS production. Moreover, H_2O_2 significantly activated and upregulated the expression of p-ERK 1/2, p-JNK, and p-P38, while edaravon protected HT22 cells against H_2O_2-induced injury by inhibiting the production of ROS and activating the MAPK signaling pathway. **Conclusions:** Our results provide the first evidence that edaravone can protect H_2O_2-induced cell injury in HT22 neurons via its antioxidant action. These findings suggest that edaravone may be useful in the treatment of neurodegenerative disorders in which oxidative stress has been principally implicated.

Introduction

The production of reactive oxygen species (ROS) and their detoxification are normal physiological processes. Nevertheless, an imbalance between ROS production and ROS removal may lead to oxidative stress. ROS are important in neuronal signaling and physiology at low levels. However, they can lead to neuronal dysfunction and cell death at higher levels [1]. Several components of ROS can cause damage to cardinal cellular components, such as lipids, proteins, and DNA, initiating subsequent cell death via necrosis or apoptosis [2]. Thus, ROS can contribute to neuronal toxicity and have been implicated in both acute injury and chronic neuropathological conditions [3]. Growing evidence from experimental models and human brain studies suggests that oxidative stress may play an important role in the common pathway for neurotoxicity in a variety of neurodegenerative diseases, including Alzheimer's disease (AD) [4], Parkinson's disease (PD)

[5], Huntington's disease (HD) [6], and amyotrophic lateral sclerosis (ALS) [7]. Therefore, the search for neuroprotective drugs that counteract ROS-induced neuronal death has attracted growing interest.

Hydrogen peroxide (H_2O_2), one of the major agents generated by oxidative stress, is produced by nearly every stage of the oxidative cycle. Neural cells that are exposed to H_2O_2 may undergo an apoptotic-like delayed death and necrosis. Substantial evidence has indicated etiological links between the generation of H_2O_2 and neurodegenerative diseases [8]. Indeed, the H_2O_2 molecule has been considered as a therapeutic target for the treatment of oxidative stress associated with these diseases. Nevertheless, the effectiveness of drugs that target this component of the disease pathology remains to be determined.

Edaravone (EDA, 3-methyl-1-phenyl-2-pyrazolin-5-one) has high liposolubility and permeability through the blood–brain barrier and is currently applied as a free radical scavenger in

the treatment of acute cerebral vascular diseases [9,10]. Some studies have demonstrated that EDA efficiently scavenges oxygen free radicals by providing a hydrogen atom [11]. Oxidative stress has been implicated as a pathogenetic mechanism for neurodegenerative diseases; thus, we suspect that EDA may be a promising therapeutic agent for oxidative stress–induced neurodegenerative disease. However, only a few reports in the literature have previously examined this possibility. To further understand the neuroprotective effects of EDA and develop its pharmaceutical application for the comprehensive management of neurodegenerative disorders, we used immortalized mouse hippocampal neurons (HT22 cells), a line possessing functional cholinergic properties and other characteristics similar to primary hippocampal neurons after differentiation [12,13], as a cell model to investigate whether EDA attenuates H_2O_2-induced neurotoxicity. Our aims were to 1) evaluate the neurocytotoxicity of H_2O_2 upon HT22 cells and 2) observe the effects of EDA on oxidative stress–induced cell death and elucidate the underlying mechanism(s) of these effects.

Materials and Methods

Materials

H_2O_2 (30%) and EDA were purchased from Merck (Darmstadt, Hessen, Germany). Fetal bovine serum (FBS) was obtained from Atlanta Biologicals (Norcross, GA, USA). A cell counting kit-8 (CCK-8) was acquired from Dojin Kagaku (Kumamoto, Kyushu, Japan). A ROS detection kit was purchased from the Beyotime Institute of Biotechnology (Guangzhou, China). Hoechst 33342 was procured from Invitrogen/Life Technologies (Carlsbad, CA, USA). The following primary antibodies were used for Western blotting: antiphospho-Erk1/2 (Thr202/Thr204), antiphospho-P38 (Thr180/Thr182), antiphospho-JNK (Thr183/Thr185), anti-Erk1/2, anti-JNK, anti-P38, and anti-Bcl-2, anti-Bax; all antibodies were purchased from Cell Signaling Technology (Danvers, MA, USA). All other routine cell culture supplies and reagents were purchased from Sigma, Invitrogen, and Fisher.

HT22 Cell Culture, Differentiation, and Treatment

HT22 cells were cultured in DMEM media supplemented with 10% FBS, 100 U/mL penicillin, and 100 μg/mL streptomycin as previously described [12]. The method used for differentiation of HT22 cells has been previously described in detail [13]. When the cell density reached 70–80%, the cells were treated with the indicated concentration of H_2O_2 for 24 h in the absence or presence of EDA (final concentrations ranged from 10 to 100 μM).

Cytotoxicity Assays

Cytotoxicity/cell viability in response to the different treatments was evaluated using a CCK-8 assay. Briefly, after each treatment, 10 μL/well of WST-8 reagent was added and the HT22 cells were incubated for 2 h at 37°C and 5% CO_2. The absorbance of the

samples was measured at 450 nm using a microplate reader with a background control as the blank. The cell survival ratio was expressed as the percentage of the control. The morphological changes were also monitored under an inverted phase contrast microscope with a digital camera.

Flow Cytometric Analysis Using annexin V and Propidium Iodide

The percentage of apoptotic cells in culture was evaluated by flow cytometric analysis using annexin V–FITC and propidium iodide (PI) fluorescence as previously described [14]. Briefly, HT22 cells were seeded in six-well plates at 2×10^5 cells/well and treated as described above. Cells were then washed twice with phosphate-buffered saline (PBS) and stained with annexin V–FITC and PI in binding buffer (10 mM Hepes, 140 mM NaCl, and 2.5 mM CaCl2). Ten thousand events were collected for each sample. The stained cells were analyzed using Cell-Quent software in the FL1-H and FL2-H channels.

In parallel with the flow cytometric analysis, Hoechst 33342 staining in living cells was performed to discriminate apoptotic cell death induced by the treatments. Highly condensed, marginalized, or fragmented chromatin in apoptotic cells is stained bright blue with Hoechst 33342 [13].

Detection of Intracellular ROS Generation

The intracellular ROS were detected by an oxidation-sensitive fluorescent probe (DCFH-DA). After treatment, the cells were washed twice in PBS, collected and adjusted to 1×10^7/ml, and incubated with DCFH-DA at 37°C for 20 min. The DCFH-DA was intracellularly deacetylated by a nonspecific esterase, which was further oxidized by ROS to produce the fluorescent compound 2,7-dichlorofluorescein (DCF). The fluorescent signal intensity of DCF was detected by FACScan flow cytometry at an excitation wavelength of 488 nm and an emission wavelength of 535 nm.

Western Blot Analysis

After treatment, the HT22 cells were lysed with an appropriate amount of boiling, denaturing lysate buffer (1% SDS, 1 mM sodium orthovanadate, 10 mM Tris-Cl, pH 7.4) supplemented with a protease inhibitor cocktail (Roche Diagnostics, Indianapolis, IN). The total protein quantification and Western blot procedures were performed routinely as previously described [15]. The following dilution rates for the different primary antibodies, all obtained from Cell Signaling Technology, were used: Bcl-2, 1:1000; Bax, 1:1000; p-JNK, 1:1000; p-P38, 1:1000; p-ERK1/2, 1:1000; JNK, 1:1000; P38, 1:500; ERK1/2, 1:2000 and GAPDH, 1:500.

Statistical Analysis

All of the statistical analyses were performed using the SPSS 11.0 software (SPSS Inc., Chicago, IL, USA). All of the data are expressed as the mean ± SE Significant differences were analyzed

with Student's *t*-test and one-way analysis of variance (ANOVA) with the significance level set at $P < 0.05$.

Results

### Morphological Changes after H_2O_2 or/and EDA Treatment

Under an inverted microscope, control HT22 cells appeared to have complete packing membranes, a normal shape and round nuclei (Figure 1A). In contrast, incomplete cellular membranes, cellular swelling, vacuole degeneration as well as pyknosis of the chromatin were observed in the H_2O_2 treatment groups. The extent of cell damage was exacerbated by the increasing level of H_2O_2. Cells treated with 1000 μM H_2O_2 were shrunken, and no cells with normal morphology could be seen (Figure 1B–D). The number of viable cells in the EDA-treated groups was increased compared to the H_2O_2 group. Cellular swelling, pyknosis of the chromatin, and vacuole degeneration in the EDA cotreatment groups were observed at a lower frequency than in the H_2O_2 group. These changes were

concentration dependent within the range of 10–60 μM EDA (Figure 1E,F).

Cell Viability after H_2O_2 or/and EDA Treatment

When the HT22 cells were treated with increasing doses of H_2O_2 for 24 h, as shown in Figure 2A, survival decreased with increasing concentrations of H_2O_2: from 84.6 $\pm$ 4.1% at 125 μM H_2O_2 to 2.87 $\pm$ 0.5% at 1000 μM H_2O_2. At 500 μM H_2O_2, approximately 40 $\pm$ 6.7% of the HT22 cells remained viable, and we selected 500 μM as the optimal dose of H_2O_2 for the subsequent experiments.

To investigate whether EDA confers protection against H_2O_2-induced cell damage in HT22 cells, we detected the cell viability of the HT22 cells after 500 μM H_2O_2 incubation for 24 h with EDA co-incubation at various concentrations from 10 to 100 μM. Our results show that cotreatment with EDA prevented the loss of cell viability induced by treatment with 500 μM H_2O_2 in a dose-dependent manner ($P < 0.05$) (Figure 2C). The application of EDA from 10 to 100 μM alone showed no cytotoxicity toward the HT22 cells (Figure 2B).
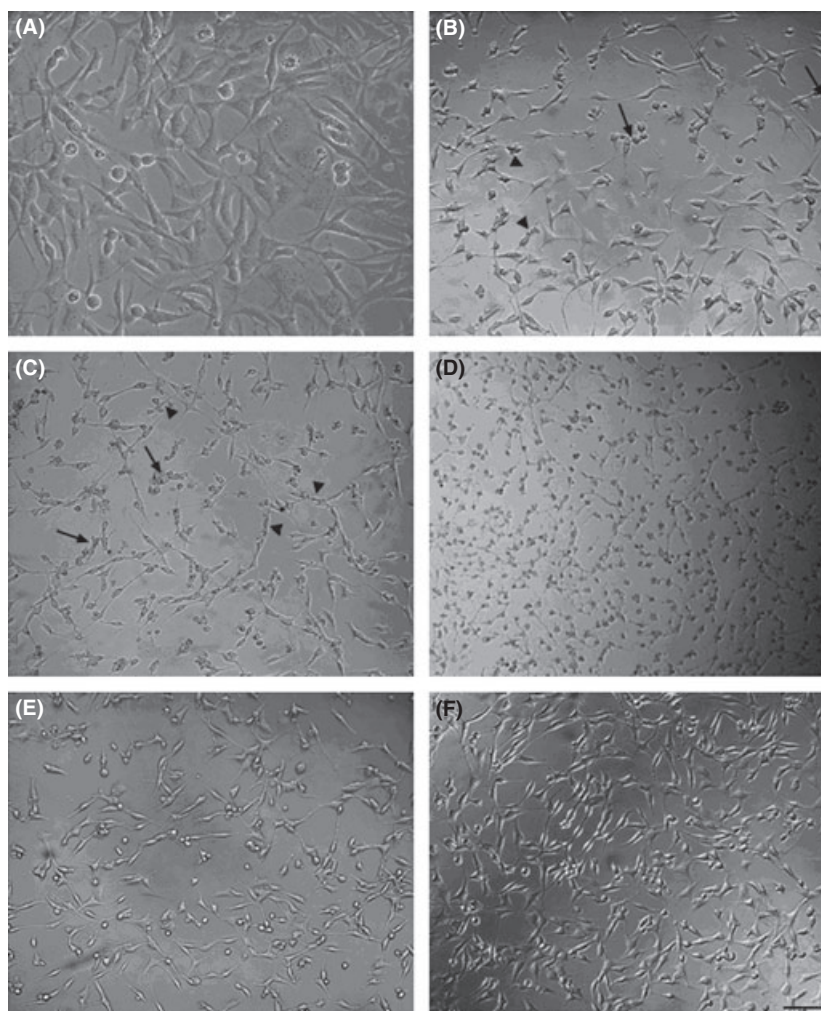

Figure 1 The effect of H_2O_2 in the absence and presence of EDA on the morphology of HT22 cells. (**A**) Normal morphologic features of HT22 cells were present in the control group (**B**–**D**). Cell morphology changed after treating with different concentrations of H_2O_2 (250 μM, 500 μM, 1000 μM). The characteristic features of an incomplete cellular membrane, cellular swelling (arrows), and vacuole degeneration were present (black triangle) (**E**, **F**). Cotreatment with EDA (30 μM, 60 μM) ameliorated H_2O_2-induced HT22 cell damage. Scale bar = 50 μm.
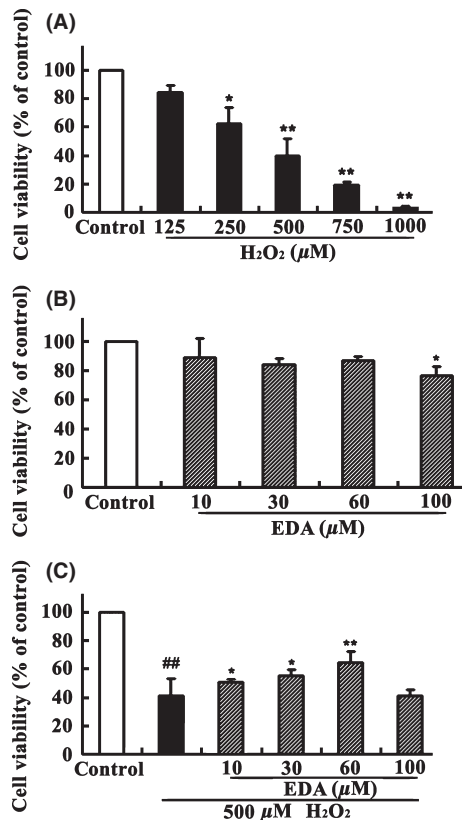
Figure 2 The protective effect of EDA on the H_2O_2-induced decrease in cell viability measured by the CCK-8 assay. (**A**) HT22 cells were incubated with different concentrations of H_2O_2 for 24 h. (**B**) HT22 cells were incubated with different concentrations of EDA for 24 h. (**C**) HT22 cells were treated with H_2O_2 (500 μM) for 24 h in the presence of various concentrations of EDA. The values represent the percentage relative to the control (no treatment) and are the mean $\pm$ SE (n $\geq$ 6). The data were analyzed using a one-way ANOVA followed by *post hoc* Tukey's multiple comparison tests. $^{\#\#}P < 0.01$ versus control, $^*P < 0.05$ and $^{**}P < 0.01$ versus H_2O_2.

H_2O_2-induced Apoptosis in HT22 Cells and Protective Effects of EDA

Apoptotic levels were quantified to examine the extent of H_2O_2-induced apoptosis and evaluate whether EDA protects against H_2O_2-induced apoptosis. The HT22 cells were incubated with different concentrations of H_2O_2 alone or in combination with EDA (10–100 μM) and H_2O_2 (500 μM) for 24 h. A flow cytometric analysis was used to quantify the rate of cell apoptosis. As shown in Figure 3, the percentage of apoptotic cells increased as the concentration of H_2O_2 increased. The apoptotic percentage was 7.61 $\pm$ 0.75% in the control group, which was significantly lower than in the H_2O_2 groups, which exhibited apoptotic rates of 37.79 $\pm$ 2.62% when treated with 250 μM H_2O_2, 45.67 $\pm$ 4.32% when treated with 500 μM H_2O_2, and 95.59 $\pm$ 0.89% when treated with 1000 μM ($P < 0.01$ or $P < 0.05$) (Figure 3A). However, EDA cotreatment clearly decreased H_2O_2-induced apoptosis. Our data show that EDA cotreatment significantly ($P < 0.05$) and dose
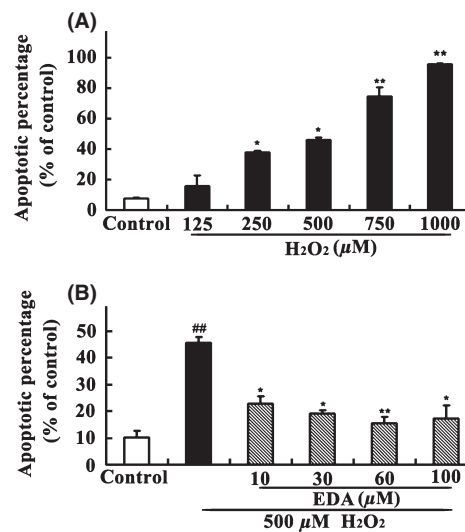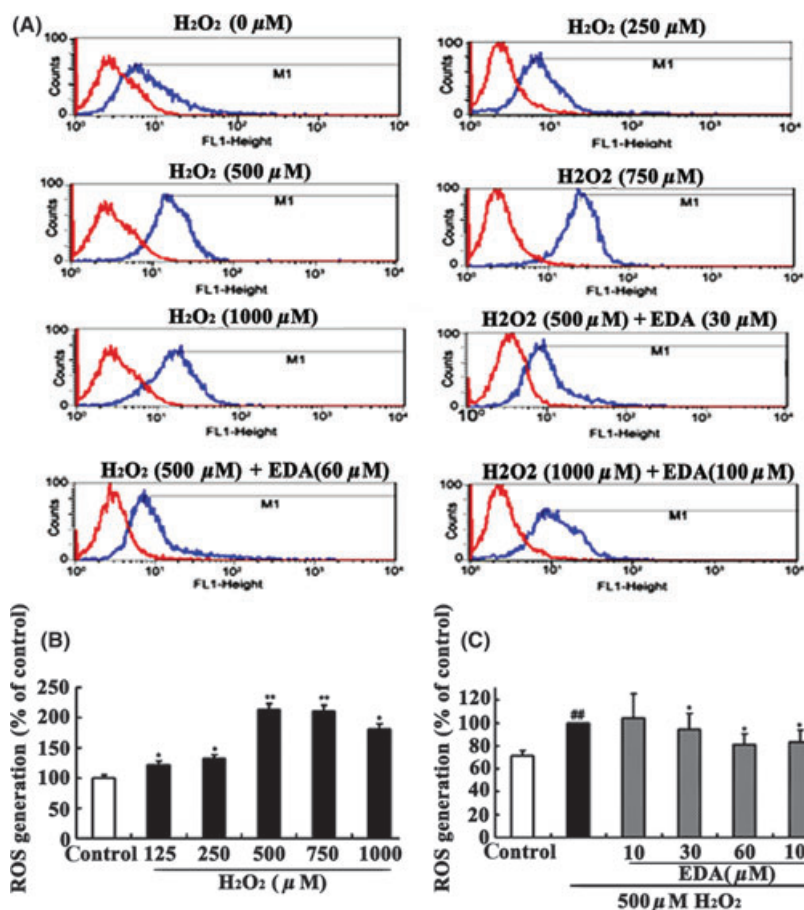

Figure 3 The protective effect of EDA against H_2O_2-induced apoptosis measured by flow cytometry. (**A**) HT22 cells were incubated with different concentrations of H_2O_2 for 24 h. (**B**) HT22 cells were treated with H_2O_2 (500 μM) for 24 h in the presence of various concentrations of EDA (10, 30, 60, 1000 μM). Cell apoptosis was assessed by flow cytometry. The values represent the percentage relative to the control and are the mean $\pm$ SE (n $\geq$ 6). The data were analyzed using a one-way ANOVA followed by *post hoc* Tukey's multiple comparison tests. $^{\#\#}P < 0.01$ versus control, $^*P < 0.05$ and $^{**}P < 0.01$ versus H_2O_2.

dependently decreased the apoptotic rate induced by H_2O_2, with a saturation at 60 μM EDA for the protective benefit (100 μM EDA showed no more protective effects compared to the 60 μM group, $P > 0.05$) (Figure 3B).

Hoechst 33342 staining revealed that the HT22 cells displayed apoptotic morphology, characterized by chromatin condensation, nuclear shrinkage, and the formation of apoptotic bodies after treatment with H_2O_2. With increasing concentrations of H_2O_2, the proportion of cells displaying apoptotic morphology gradually increased. In cells treated with 1000 μM H_2O_2, normal nuclear morphology was rarely observed. However, cotreatment with EDA reduced the apoptotic fraction of HT22 cells. This observation was consistent with the results obtained from the CCK-8 assay and flow cytometry. Taken together, these findings suggest that EDA is capable of attenuating H_2O_2-induced cell apoptosis.

EDA Inhibited the Generation of ROS Induced by H_2O_2 in HT22 Cells

To elucidate the effects of EDA on H_2O_2-induced oxidative stress, the levels of ROS production in cells were measured using the fluorescence probe DCF. In H2DCF-DA-loaded HT22 cells, H_2O_2 application increased the fluorescence intensity, indicating the generation of ROS. After exposing the cells to H_2O_2 for 24 h, the M1 peak gradually shifted to the right (Figure 4A), indicating that the ROS production gradually increased with increasing concentrations of H_2O_2. Moreover, HT22 cells treated with 500 μM H_2O_2 for 24 h exhibited an approximately 2-fold increase in fluorescence intensity compared to the control group (Figure 4B).

Figure 4 The protective effect of EDA on H_2O_2-induced ROS generation measured by flow cytometry. HT22 cells treated with different concentrations of H_2O_2 in the absence and presence of EDA were loaded with H_2DCF-DA to detect the generation of intracellular ROS. (**A**) The M_1 peak gradually shifted to the right compared to the control group. However, the M_1 peak shifted to the left compared to the H_2O_2 group when the cells were co-incubated with EDA. (**B**) H_2O_2 significantly increased the intracellular level of ROS compared to the control group (**$**P < 0.01$ or *$P < 0.05$). (**C**) Cotreatment with EDA reduced the levels of ROS ($P < 0.05$ compared to the H_2O_2 group). The values represent the percentage relative to the control (no treatment) and are the mean $\pm$ SE (n $\geq$ 6). The data were analyzed by a one-way ANOVA followed by *post hoc* Tukey's multiple comparison tests. $^{\#\#}P < 0.01$ versus control,*$P < 0.05$ and **$P < 0.01$ versus H_2O_2.

Furthermore, our data show that cotreatment with EDA significantly inhibited the elevated intracellular levels of ROS induced by H_2O_2 in a significant ($P < 0.05$), dose-dependent manner.

EDA Inhibited MAPK Family Activation Stimulated by H_2O_2

To further explore the mechanism of the protective effects of EDA, we next examined the effect of EDA on potential pathways that are activated during apoptosis. We first examined the protein expression levels of Bcl-2 and Bax. As shown in Figure 5, H_2O_2 treatment resulted in decreased Bcl-2 expression and increased Bax expression compared to the control groups, a tendency that was reversed by EDA cotreatment. Moreover, previous studies have demonstrated that H_2O_2-induced oxidative stress may trigger apoptosis by activation of mitogen-activated protein kinase (MAPK) pathways [16,17]. To clarify the mechanism of action underlying EDA protection, MAPK activities were investigated using Western blot analysis. Compared to the control group, we found that treating the HT22 cells with H_2O_2 for 24 h increased the phosphorylation of ERK1/2, JNK1/2, and P38 in a concentration-dependent manner. However, cotreatment with EDA decreased the expression levels of p-JNK, p-P38, and p-ERK1/2 (Figure 6). These results suggest that EDA protects HT22 cells against H_2O_2-induced oxidative injury by inhibiting the phosphorylation of MAPK pathway members.

Discussion

Oxidative stress refers to the cytologic consequences of a mismatch between the production of free radicals and the ability of the cell to defend against them. Substantial data have been assembled to investigate the essential role of oxidative stress in the regulation of diverse cellular events such as proliferation, differentiation, adhesion, oxidative damage, and cell death [18,19]. Several components of ROS, such as H_2O_2, may lead to various forms of reversible and irreversible oxidative modification of proteins, lipids, and DNA, initiating subsequent cell death via necrosis or apoptosis and leading to cellular damage [2,20].

A number of oxidants are produced as by-products of normal aerobic cell metabolism, and ROS levels are particularly high in neurodegenerative disorders. The central nervous system is especially vulnerable to oxidative stress due to the relatively low levels of cellular antioxidants, high oxygen consumption, and high concentrations of lipids and metal cations available for the generation of free radicals [21]. Thus, oxidative stress has been considered to be one of the major risk factors to exacerbate neuronal damage, via different molecular pathways, in many neurodegenerative disorders. Currently, there is growing evidence showing that oxidative stress induced by ROS or free radicals plays a key role in the pathogenesis of neurodegenerative disorders, including AD, PD, HD, and amyotrophic lateral sclerosis [4–7,22]. Therefore, the removal of excess ROS or the suppression of their generation by
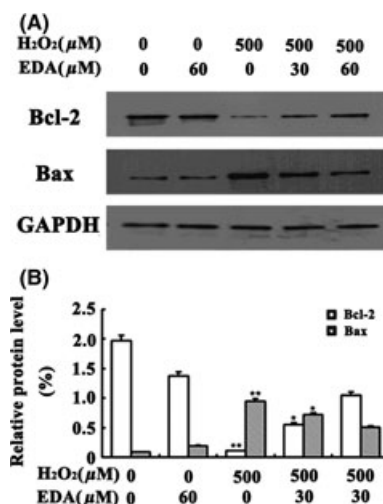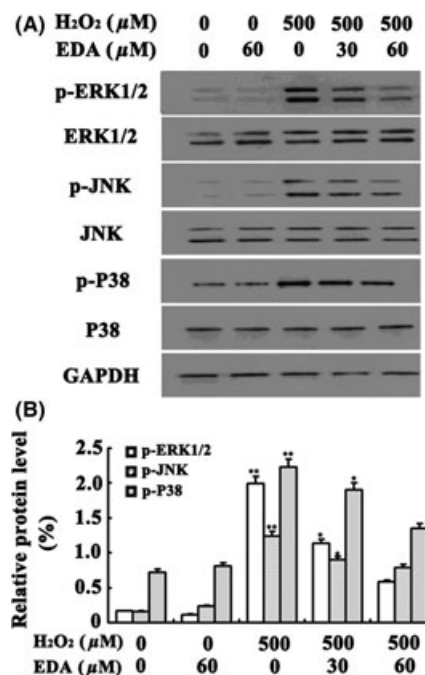
Figure 5 The effects upon Bcl-2 and Bax expression following EDA treatment. HT22 cells were treated with 500 μM H_2O_2 and cotreated with different concentrations of EDA for 24 h. Then, the cells were harvested and assayed for the expression of Bcl-2 and Bax. The results are presented as the mean $\pm$ SE from at least three independent experiments. The expression of GAPDH confirms equal protein loading. Panel A shows the protein expression in the HT22 cells. Panel B depicts the statistical results (**$P < 0.01$, *$P < 0.05$).

Figure 6 The effects upon ERK, JNK, and P38 expression following EDA treatment. HT22 cells were treated with 500 μM H_2O_2 and cotreated with different concentrations of EDA for 24 h. Then, the cells were harvested and assayed for the expression of p-ERK1/2, p-JNK1/2, and p-P38. The results are presented as the mean $\pm$ SE from at least three independent experiments. The expression of GAPDH confirms equal protein loading. Panel A shows the protein expression in the HT22 cells. Panel B depicts the statistical results (**$P < 0.01$, *$P < 0.05$).

antioxidants may be effective in preventing degeneration of neural cells.

H_2O_2, formed as a natural by-product of enzymatic oxidase action, is an endogenous source of hydroxyl free radicals normally produced in cells, including neurons. Exogenous H_2O_2 is able to cross membranes and thus directly alter the intracellular concentration. Furthermore, H_2O_2 is a major ROS that can induce oxidative stress by increasing the production of other ROS, subsequently leading to cell damage and death. Moreover, H_2O_2 is involved in the regulation of a variety of cellular events, such as cell proliferation, signal transduction, DNA damage, and cell apoptosis [20,21]. Therefore, H_2O_2 has been extensively used as an inducer of neuronal injury to both explore the mechanisms of oxidative stress and evaluate the neuroprotective potential of new pharmacotherapies [23]. In this study, we also used H_2O_2 to generate an *in vitro* model of oxidative stress.

Edaravone, a lipophilic molecule with rapid access to the intracellular space, is a powerful free radical scavenger that has been clinically used to reduce neuronal damage following cerebral ischemic stroke [9,10]. It protects cells from injury by directing the scavenging activities of the hydroxy radical (OH·) and inhibiting lipoxygenase activity and 15-HPETE. Furthermore, it can also directly neutralize peroxy radicals (LOO·) but does not scavenge for O_2· [24]. Consequently, EDA has been evaluated as a neuroprotective compound [25]. Recently, EDA has been offered as a viable candidate for the treatment of oxidative stress–induced neurodegenerative disease [26,27], but until now, research on its effect and probable mechanisms in the treatment of such diseases was lacking. Therefore, in this study, we attempted to verify the antioxidative role of EDA in a hippocampal cell model of oxidative injury.

Our results provide direct evidence of EDA protection against H_2O_2-induced HT22 cell injury based on the CCK-8 method. Exogenous H_2O_2 decreased cell viability in a concentration-dependent manner, and 500 μM H_2O_2 caused a significant decrease 40 $\pm$ 6.7% in HT22 cell viability. However, cotreatment with EDA for 24 h increased cell viability in a concentration-dependent manner. As an extension of the cell viability results, we evaluated cell apoptosis and the generation of ROS. When HT22 cells were exposed to H_2O_2, cell apoptosis and ROS levels increased. In contrast, cotreatment with EDA decreased both the apoptotic rate of HT22 cells and the production of ROS generation. These protective effects may contribute to the antioxidative activity of EDA.

After discovering that EDA exerted a protective effect against H_2O_2-induced cytotoxicity in HT22 cells, we studied the potential pathway responsible for these effects. The MAPKs, a family of serine/threonine protein kinases, are involved in many cellular processes, including cell growth, differentiation, inflammation, and cell death [28]. MAPKs are key kinases in signal transduction pathways, and members of each major MAPK subfamily (JNK, P38, and ERK1/2) have been implicated in neuronal injury and disease [29]. The unphosphorylated forms of the MAPKs are virtually inactive, and phosphorylation stimulates their activity. The oxidative stress–induced ROS activation of JNK, ERK1/2, and/or P38 has been described in various types of

cells, and ROS activation of the MAPK cascade might be a common mechanism by which oxidative stress induces neuronal cell death or neurodegenerative disorders [30,31]. In this study, we examined the expression of the three signaling proteins in the MAPK pathway. We found that activation of JNK, P38, and ERK1/2 in HT22 cells was significantly increased following exposure to H_2O_2, a result which is consistent with studies on other cell models [32,33]. However, when the cells were cotreated with EDA, activation of the MAPKs was reduced, suggesting that EDA protects cells from oxidative stress–induced apoptosis by inhibiting the MAPK signaling pathway.

Taken together, our results demonstrate that H_2O_2 can induce cell apoptosis through the production of ROS and activation of the MAPK signaling pathway. To the best of our knowledge, we show for the first time that EDA, a radical scavenger, can inhibit the production of ROS and the expression of the MAPK signaling pathway and thus confer protection for HT22 cells [34]. Currently, many studies suggest that oxidative stress–induced damage is involved in many neurodegenerative diseases, including AD.

Thus, antioxidant treatment may be an effective method for the treatment of these diseases. As a radical scavenger, EDA has been used to treat brain stroke/ischemia, and as shown in our study, it can also protect HT22 cells from H_2O_2-induced cell apoptosis, indicating its potential as an antioxidant candidate in the treatment of neurodegenerative diseases.

Acknowledgments

Conflict of Interest

The authors declare no conflict of interest.

References

1. Berlett BS, Stadtman ER. Protein oxidation in aging, disease, and oxidative stress. *J Biol Chem* 1997;**272**:20313–20316.

2. Gorman AM, McGowan A, O'Neill C, Cotter T. Oxidative stress and apoptosis in neurodegeneration. *J Neurol Sci* 1996;**139**(Suppl):45–52.

3. Pettmann B, Henderson CE. Neuronal cell death. *Neuron* 1998;**20**:633–647.

4. Choi J, Sullards MC, Olzmann JA, et al. Oxidative damage of DJ-1 is linked to sporadic Parkinson and Alzheimer diseases. *J Biol Chem* 2006;**281**:10816–10824.

5. Caviness JN, Lue L, Adler CH, Walker DG. Parkinson's disease dementia and potential therapeutic strategies. *CNS Neurosci Ther* 2011;**17**:32–44.

6. Stoy N, Mackay GM, Forrest CM, et al. Tryptophan metabolism and oxidative stress in patients with Huntington's disease. *J Neurochem* 2005;**93**:611–623.

7. Bellingham MC. A review of the neural mechanisms of action and clinical efficiency of riluzole in treating amyotrophic lateral sclerosis: What have we learned in the last decade? *CNS Neurosci Ther* 2011;**17**:4–31.

8. Ishikawa Y, Satoh T, Enokido Y, Nishio C, Ikeuchi T, Hatanaka H. Generation of reactive oxygen species, release of L-glutamate and activation of caspases are required for oxygen-induced apoptosis of embryonic hippocampal neurons in culture. *Brain Res* 1999;**824**:71–80.

9. Edaravone Acute Infarction Study Group. Effect of a novel free radical scavenger, edaravone (MCI-186), on acute brain infarction. Randomized, placebo-controlled, double-blind study at multicenters. *Cerebrovasc Dis* 2003;**15**:222–229.

10. Yang J, Liu M, Zhou J, Zhang S, Lin S, Zhao H. Edaravone for acute intracerebral haemorrhage. *Cochrane Database Syst Rev* 2011:CD007755.

11. Kawasaki T, Kitao T, Nakagawa K, et al. Nitric oxide-induced apoptosis in cultured rat astrocytes: Protection by edaravone, a radical scavenger. *Glia* 2007;**55**:1325–1333.

12. Liu J, Li L, Suo WZ. HT22 hippocampal neuronal cell line possesses functional cholinergic properties. *Life Sci* 2009;**84**:267–271.

13. Zhao Z, Lu R, Zhang B, et al. Differentiation of HT22 neurons induces expression of NMDA receptor that mediates homocysteine cytotoxicity. *Neurol Res* 2012;**34**:38–43.

14. Luan P, Zhou H, Zhang B, et al. Basic Fibroblast Growth Factor Protects C17.2 Cells from Radiation-induced Injury through ERK1/2. *CNS Neurosci Ther* 2012;**18**:767–772.

15. Liu J, Rasul I, Sun Y, et al. GRK5 deficiency leads to reduced hippocampal acetylcholine level via impaired presynaptic M2/M4 autoreceptor desensitization. *J Biol Chem* 2009;**284**:19564–19571.

16. Valencia A, Moran J. Reactive oxygen species induce different cell death mechanisms in cultured neurons. *Free Radic Biol Med* 2004;**36**:1112–1125.

17. Ruffels J, Griffin M, Dickenson JM. Activation of ERK1/2, JNK and PKB by hydrogen peroxide in human SH-SY5Y neuroblastoma cells: Role of ERK1/2 in H_2O_2-induced cell death. *Eur J Pharmacol* 2004;**483**:163–173.

18. Bergamini CM, Gambetti S, Dondi A, Cervellati C. Oxygen, reactive oxygen species and tissue damage. *Curr Pharm Des* 2004;**10**:1611–1626.

19. Martindale JL, Holbrook NJ. Cellular response to oxidative stress: Signaling for suicide and survival. *J Cell Physiol* 2002;**192**:1–15.

20. Giorgio M, Trinei M, Migliaccio E, Pelicci PG. Hydrogen peroxide: A metabolic by-product or a common mediator of ageing signals? *Nat Rev Mol Cell Biol* 2007;**8**:722–728.

21. Brown DR, Schmidt B, Kretzschmar HA. Effects of oxidative stress on prion protein expression in PC12 cells. *Int J Dev Neurosci* 1997;**15**:961–972.

22. He F, Luan P, He R, et al. Effect of edaravone on Aβ1-40 induced enhancement of voltage-gated calcium channel current. *CNS Neurosci Ther* 2012;**18**:89–90.

23. Saitoh M, Nishitoh H, Fujii M, et al. Mammalian thioredoxin is a direct inhibitor of apoptosis signal-regulating kinase (ASK) 1. *EMBO J* 1998;**17**:2596–2606.

24. Watanabe T, Yuki S, Egawa M, Nishi H. Protective effects of MCI-186 on cerebral ischemia: Possible involvement of free radical scavenging and antioxidant actions. *J Pharmacol Exp Ther* 1994;**268**:1597–1604.

25. Kaur C, Ling EA. Antioxidants and neuroprotection in the adult and developing central nervous system. *Curr Med Chem* 2008;**15**:3068–3080.

26. Pan YH, Wang YC, Zhang LM, Duan SR. Protective effect of edaravone against PrP106-126-induced PC12 cell death. *J Biochem Mol Toxicol* 2010;**24**:235–241.

27. Xiong N, Xiong J, Khare G, et al. Edaravone guards dopamine neurons in a rotenone model for Parkinson's disease. *PLoS ONE* 2011;**6**:e20677.

28. Pearson G, Robinson F, Beers GT, et al. Mitogen-activated protein (MAP) kinase pathways: Regulation and physiological functions. *Endocr Rev* 2001;**22**:153–183.

29. Harper SJ, Wilkie N. MAPKs: New targets for neurodegeneration. *Expert Opin Ther Targets* 2003;**7**:187–200.

30. Ouyang M, Shen X. Critical role of ASK1 in the 6-hydroxydopamine-induced apoptosis in human neuroblastoma SH-SY5Y cells. *J Neurochem* 2006;**97**:234–244.

31. Kim SD, Moon CK, Eun SY, Ryu PD, Jo SA. Identification of ASK1, MKK4, JNK, c-Jun, and caspase-3 as a signaling cascade involved in cadmium-induced neuronal cell apoptosis. *Biochem Biophys Res Commun* 2005;**328**:326–334.

32. Kim SK, Woodcroft KJ, Oh SJ, Abdelmegeed MA, Novak RF. Role of mechanical and redox stress in activation of mitogen-activated protein kinases in primary cultured rat hepatocytes. *Biochem Pharmacol* 2005;**70**:1785–1795.

33. Yeo JE, Kim JH, Kang SK. Selenium attenuates ROS-mediated apoptotic cell death of injured spinal cord through prevention of mitochondria dysfunction; in vitro and in vivo study. *Cell Physiol Biochem* 2008;**21**:225–238.

34. Inokuchi Y, Imai S, Nakajima Y, et al. Edaravone, a free radical scavenger, protects against retinal damage in vitro and in vivo. *J Pharmacol Exp Ther* 2009;**329**:687–698.